

# Structure–property relationships of nanocomposite-like polymer blends with ultrahigh viscosity ratios

J.K. Rameshwaram<sup>a</sup>, Y.-S. Yang<sup>b,\*</sup>, H.S. Jeon<sup>a,\*</sup>

<sup>a</sup>Department of Petroleum and Chemical Engineering, New Mexico Institute of Mining and Technology, 801 Leroy Place, Socorro, NM 87801, USA

<sup>b</sup>Department of Mechanical Engineering, Chonnam National University, Kwang-Ju, South Korea

Received 21 January 2005; received in revised form 3 May 2005; accepted 5 May 2005

Available online 26 May 2005

## Abstract

We have investigated the structure–property relationships and the effects of a viscosity ratio on the rheological properties of nanocomposite-like polymer blends using oscillatory and steady shear rheometry and optical microscopy. These immiscible blends are consisted of ultrahigh viscous polybutadiene (PB1), high viscous polybutadiene (PB2), and low viscous polydimethylsiloxane (PDMS). The PB1/PDMS blends with an ultrahigh viscosity ratio ( $\lambda=162,000$ ) exhibit non-Newtonian fluids behavior for  $\Omega \geq 0.1$  while the PDMS/PB2 blends ( $\lambda=37$ ) exhibit pseudo-Newtonian fluids behavior for  $\Omega > 0.6$ , where  $\Omega$  is the weight fraction of PB1 or PB2 in the blends. The viscoelastic properties of the PB1/PDMS blends increase systematically with an increasing the weight fraction of PB1, and then exhibit plateau values above a certain maximum weight fraction ( $\Omega_m$ ) of PB1. In addition the viscoelastic properties of the PB1/PDMS blends are not affected by the change of blend morphology or phase inversion, where  $\Omega_m$  is larger than the phase inversion weight fraction ( $\Omega_p$ ). In contrast the viscoelastic properties of the PB2/PDMS blends follow a positive-deviation mixing rule and are significantly affected by phase inversion. © 2005 Elsevier Ltd. All rights reserved.

**Keywords:** Immiscible blend; Nanocomposite-like polymer blend; Ultrahigh viscosity ratio

## 1. Introduction

The blending of immiscible or miscible polymers has become an increasingly important technique for developing the cost-effective commercial materials. Polymer blends are physical mixtures of two or more polymers and have been commercialized as immiscible or miscible systems [1,2]. In these mixtures, most of commercial polymers tend to separate into two or more distinct phases due to incompatibility. It is much more cost-effective to blend two or more polymers with known properties than to synthesize new polymers having unknown properties. A specific example of such systems in which immiscibility is beneficial for the impact modification of brittle polystyrene by rubber is acrylonitrile–butadiene–styrene (ABS) or high impact polystyrene (HIPS).

Therefore, the advantages of immiscible polymer blends

are similar to those for the development of polymer composites. In particular, the viscoelastic behavior of the polymer blend with an ultrahigh viscosity ratio may be similar to those of polymer nanocomposites. While the structure and properties of immiscible polymer blends have been studied extensively [1–22], in spite of the commercial importance, there are virtually no data on the composite-like polymer blends with extremely high viscosity ratios.

In this paper, we have studied the effects of a viscosity ratio on the rheological properties of the nanocomposite-like polybutadiene (PB1)/polydimethylsiloxane (PDMS) blend with an extremely high viscosity ratio ( $\lambda=162,000$ ) and the immiscible polybutadiene (PB2)/PDMS blend with a high viscosity ratio ( $\lambda=37$ ) as a function of various compositions. We also have investigated the relationships between blend morphology and viscoelastic properties and the effects of phase inversion on viscoelastic properties using oscillatory and steady shear rheometry and optical microscopy. To study the deformation or breakup effect of dispersed domains on the rheological properties, we performed steady and oscillatory shear measurements with and without pre-shear which changes the morphology of the blends [5,6,24]. We used a very high viscosity PB1

\* Corresponding authors.

E-mail address: [jeon@nmt.edu](mailto:jeon@nmt.edu) (H.S. Jeon).

( $\eta_0=487,000$  Pa s), a high viscosity PB2 ( $\eta_0=1100$  Pa s) and a low viscosity PDMS ( $\eta_0=30$  Pa s). In general, one would not expect the breakup of dispersed domains to occur in a blend with a viscosity ratio larger than 4 [23].

In general, the storage modulus of immiscible or phase separated blends in low frequencies (or terminal regime) shows unusual terminal responses [24,25]. However, we did not observe any significant deviation from a typical terminal response due to the interfacial tension between the two phases, rather, observed the viscoelastic behavior similar to those of polymer/clay nanocomposites [26–28] over the wide range of frequencies ( $0.1 < \omega < 100$  rad/s); the viscoelastic properties of the PB/PDMS blends such as viscosity and storage and loss moduli exhibit pseudo solid-like behavior at low frequencies as well as increase significantly at high frequencies. We also find a critical composition of PB1 in the PB1/PDMS blends above which the viscoelastic properties are dominated not by phase inversion but by the contribution of the PB1 component. Therefore, the polymer blend consisted of PB1 and PDMS can be considered as a good model system for the study of polymer nanocomposites owing to the ultrahigh viscosity ratio of the PB1/PDMS blend ( $\lambda=162,000$ ).

## 2. Experimental section

### 2.1. Materials

The polymers that were used in this study have been selected in order to study the effects of a viscosity ratio on the rheological properties of the immiscible polymer blends having high viscosity ratios. We selected an ultrahigh viscosity polybutadiene homopolymer (PB1), a high viscosity polybutadiene homopolymer (PB2), and a low viscosity polydimethylsiloxane homopolymer (PDMS). PB1 and PB2 were synthesized by sequential anionic polymerization under high vacuum in hydrocarbon solvents at 25 °C with *sec*-butyl lithium as the initiator and isopropanol as the terminator [29]. Standard high vacuum procedures were used to purify the reagents [30]. The PDMS homopolymer used in this study was purchased from Aldrich and used as received. The number-average molecular weight ( $M_n$ ), the weight-average molecular weight ( $M_w$ ) and the polydispersity of polybutadiene polymers were determined by gel permeation chromatography (GPC). The microstructure was probed using  $^{13}\text{C}$  nuclear magnetic resonance (NMR). The polybutadiene chains are statistical copolymers, composed of 1–4, 1–2 isomers. The polybutadiene homopolymers with ultrahigh ( $\eta_0=487,000$  Pa s) and high ( $\eta_0=1100$  Pa s) viscosity are denoted as PB1 and PB2, respectively. The results of the polymer characterization are summarized in Table 1.

### 2.2. Sample preparation

The immiscible polymer blends of PB1/PDMS (J-series) and PB2/PDMS (K-series) were prepared via solution blending [5,24]. The PB1/PDMS and PB2/PDMS blends are labeled as  $J_x$  and  $K_x$ , respectively, where  $x$  is the weight fraction of PB1 or PB2 in the blends. The exact compositions and designations of these blends used in this study are given in Table 2. All experiments were performed at a constant temperature of 70 °C, where the blends show two-phase structures under quiescent conditions. The blend sample was heated from room temperature to 70 °C and held for 5 min under quiescent or pre-shear ( $\dot{\gamma}=0.01$  or  $0.1\text{ s}^{-1}$ ) condition to obtain the reproducible initial two-phase morphology for each sample. The samples for optical microscopy were prepared by spin coating the diluted solutions (5% concentration in cyclohexane) on quartz substrates at 2300 rpm for 30 s and then dried in a vacuum oven. These spin-coated samples were heated to a temperature 70 °C under vacuum and the morphology of these samples at this temperature was frozen in liquid nitrogen instantaneously in order to retain the morphology.

### 2.3. Rheometer

The instrument used for the rheological measurements is PHYSICA UDS 200 rheometer. All experiments were carried out with a 25 or 50 mm diameter fixture and 0.4 mm gap thickness for oscillatory and steady shear measurements. All rheological measurements for the PB1/PDMS (J-series) and PB2/PDMS (K-series) blends were performed at a fixed temperature of 70 °C under an atmosphere of nitrogen gas flow to prevent any thermal degradation of the polymers which are known to be sensitive to heat [24]. In order to study the linear viscoelastic properties, we performed the oscillatory shear measurements ranging from 0.1 to 100 rad/s in a constant strain mode with small strain amplitude, ( $\gamma=0.1$ ). The measurements were performed with a time delay of 5 min after cessation of three different steady pre-shears (0, 0.01 or  $0.1\text{ s}^{-1}$ ) in order to make sure that we are measuring the viscoelastic properties of the blends after the relaxation of the deformed structure of the dispersed phase in the blend.

## 3. Results and discussion

### 3.1. Rheological properties of homopolymers

Fig. 1 shows the dynamic viscosity for three homopolymers (PB1, PB2, and PDMS). The higher molecular weight polymer PB1 shows a shear thinning behavior over the wide range of a shear rate, while the relatively lower molecular weight polymers PB2 and PDMS show Newtonian fluids behavior. The zero-shear viscosity ( $\eta_0$ ) of the PB1, PB2, and PDMS homopolymers are 487,000, 1100,

Table 1  
Characterization data of three homopolymers

Samples	$M_w$ (g/mol)	$M_w/M_n$	$\eta_0$ (Pa s)	Microstructure (mol%)		
				1, 4	1, 2	3, 4
PB1	160,000	~2.8	487,000	93	7	0
PB2	65,000	1.1	1100	91	9	0
PDMS	94,000	~3.1	30	–	–	–

and 30 Pa s, respectively. The homopolymer PB1 can be considered as solid particles dispersed in the PDMS fluids such as suspensions or composites because its viscosity is much larger than that of PDMS; the viscosity ratio of PB1 to PDMS is 162,000.

Fig. 2(a) and (b) shows the storage modulus ( $G'$ ) and loss modulus ( $G''$ ) for three homopolymers (PB1 and PB2, and PDMS). For the PB2 and PDMS homopolymers, the slopes of  $\log G'$  vs.  $\log \omega$  and  $\log G''$  vs.  $\log \omega$  (or power-law equations) are close to 2 and 1, respectively, similar to the characteristic behavior of a monodisperse polymer in the terminal regime. In contrast, for the higher molecular weight PB1, the slope in  $G'$  is much smaller than 2 and close to 0.5 whereas the slope in  $G''$  is smaller than 1 and similar to 0.5 in the terminal regime of low frequencies. The experimental values of the slope (or power-law exponents) for  $G'$  obtained from other phase separated or immiscible polymer blends vary between 0.5 and 1 [10]. The small values of these exponents suggest that the high molecular weight PB1 may have phase-separated microstructure in a molecular level and has a broad distribution in molecular weight. The loss modulus also shows similar behavior observed in storage modulus.

### 3.2. PB1/PDMS blends with ultrahigh viscosity ratio ( $\lambda = 162,000$ )

Fig. 3 shows optical micrographs of two-phase PB1/PDMS blends under quiescent conditions. The dispersed

phase of PB1 appears as bright domains while the continuous phase of PDMS is shown as dark color in the J10, J20, and J30 blends. In contrast, for the J40, J50, and J60 blends, the dispersed PDMS domains are shown as dark color. Thus, the phase inversion weight fraction would be  $\Omega_p = 0.35 \pm 0.05$  for the PB1/PDMS (J-series) blends at a quiet condition. In particular, we should note the small droplets dispersed at the inside of the bright PB1 domains in the J20 and J30 blends. It is probably because the continuous PDMS phase having much smaller viscosity tends to break up into small droplets and diffuse into the large PB1 domains.

We observed that the PB1 is the dispersed phase in the blends up to the phase inversion composition, which is the changing of the dispersed phase into the continuous phase or the continuous phase into the dispersed phase. This occurs with an increase in the concentration of the dispersed phase. Phase inversion in two-phase polymer blends is a key factor that can influence domain morphology in a number of practical applications [1,2,31–35]. Phase inversion occurs when the dispersed phase is converted into a continuous phase due to changes in concentration, temperature, and/or shear forces. An empirical equation that predicts the point at which phase inversion will occur in terms of a dimensionless parameter  $\beta$  has been reported [36–38];

$$\beta = \frac{\phi_A \eta_A}{\phi_B \eta_B} \quad (1)$$

where  $\phi_i$  is the volume fraction of component  $i$  ( $i = A$  or  $B$ )

Table 2  
Characterization data of immiscible PB1/PDMS (J-series) and PB2/PDMS (K-series) blends

Blend	Weight fraction (PB1 or PB2)	Dispersed phase	$\eta_0^*$ (Pa s) <sup>a</sup>	$G'_0$ (Pa) <sup>a</sup>	$G''_0$ (Pa) <sup>a</sup>
J1	0.01	PB1	28	–	2.8
J10	0.1	PB1	4410	323	300
J20	0.2	PB1	24,000	1790	1600
J30	0.3	PB1	152,840	11,200	10,400
J40	0.4	PDMS	150,230	11,300	9900
J50	0.5	PDMS	129,530	9430	8880
J60	0.6	PDMS	201,660	15,500	12,900
J70	0.7	PDMS	161,070	12,300	10,400
J80	0.8	PDMS	229,730	17,900	14,400
K10	0.1	PB2	60	0.28	5.9
K30	0.3	PB2	79	1.07	16.0
K50	0.5	PB2	221	2.17	32.0
K70	0.7	PB2	777	14.2	76.4
K90	0.9	PDMS	1091	5.41	109.0

<sup>a</sup> The zero-shear rate viscoelastic properties of the blends were obtained at  $\omega = 0.1$  rad/s.

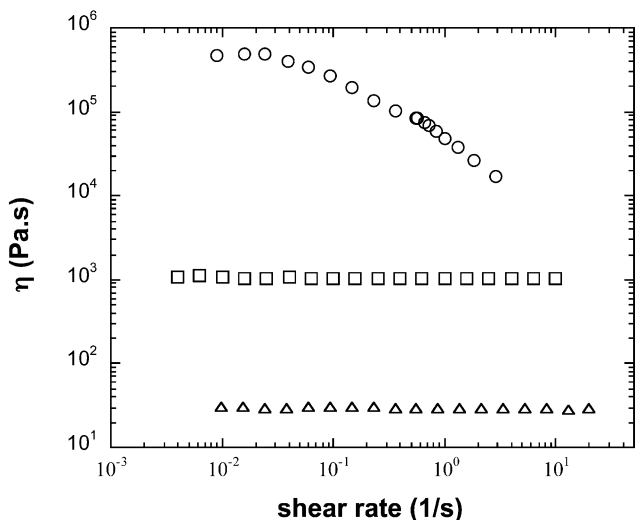


Fig. 1. Dynamic viscosity of three homopolymers. Symbols: PB1 (circles), PB2 (squares), and PDMS (triangles).

and  $\eta_i$  represents the viscosity of component  $i$  at a given shear rate and temperature. This equation implies that the viscosity and composition ratio of the two components determine the phase inversion composition. If  $\beta$  is smaller than 1.0, the A-rich phase is dispersed while if  $\beta$  is larger than 1.0, the B-rich phase is dispersed. If the viscosity ratio is balanced by the composition ratio ( $\beta=1$ ), then phase inversion may occur under either quiescent or shear conditions. Several studies have demonstrated that Eq. (1) has validity both for blends with viscosity ratios close to unity [37–39]. In contrast, Eq. (1) does not quantitatively predict the correct phase inversion point for systems that exhibit viscous or viscoelastic asymmetry between the components of blends or mixtures [2,33,40–42]. In general, the morphology of polymer blends is affected by such things as processing conditions, composition, and the viscoelastic properties of both phases, as well as the interfacial tension between them. Eq. (1) implies that phase inversion depends not only on thermodynamic variables (such as volume fraction and temperature), but also on hydrodynamics via the shear viscosity. The phase inversion composition may not be coincided with a discontinuity in the viscoelastic properties of polymer blends with viscous or viscoelastic asymmetry.

Fig. 4 shows the dynamic viscosity ( $\eta'$ ) of the PB1/PDMS blends for a wide range of PB1 weight fractions (0.01–0.8). The blends exhibit Newtonian fluids behavior for the J1 blend at all frequencies. In contrast the dynamic viscosity of the other blends is characterized as shear-thinning fluids at all frequencies, and the slope ( $n$ ) of  $\log \eta'$  vs.  $\log \omega$  can be expressed with a power-law equation ( $\eta' \sim \omega^{-n}$ ). In the low frequency regime, the slope is close to  $-0.5$  for all blends except the J1 blend. We see systematic large increases in the viscosity with an increasing PB1 concentration until  $\Omega=0.3$  while it slightly increases with an increasing the weight fraction of PB1 from 0.3 to 0.8.

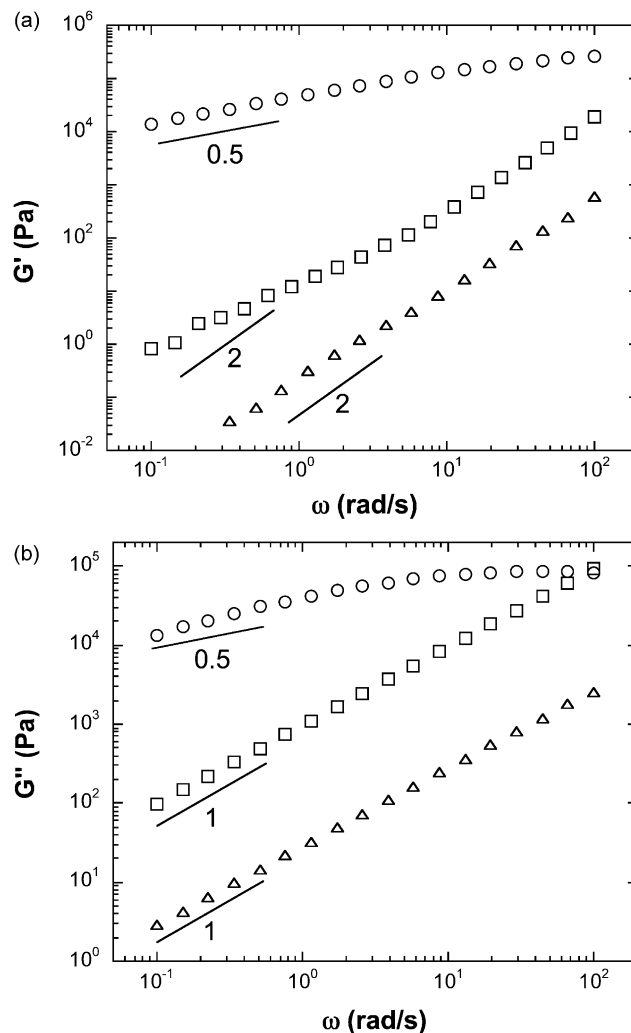


Fig. 2. (a) Dynamic storage modulus of three homopolymers. Symbols: PB1 (circles), PB2 (squares), and PDMS (triangles). (b) Dynamic loss modulus of three homopolymers. Symbols: PB1 (circles), PB2 (squares), and PDMS (triangles).

Fig. 5(a) and (b) shows the storage and loss modulus at the various weight fraction of PB1 ( $\Omega=0.01, 0.1, 0.2, 0.3, 0.4, 0.5, 0.6, 0.7,$  and  $0.8$ ). For  $\Omega \geq 0.1$  we see big jumps compared to the storage or loss modulus of the J1 blend at low frequencies ( $\omega < \sim 1$  rad/s). In particular we see large enhancements in  $G'$  at least 5 orders of magnitude at the low frequencies. In contrast, the storage and loss moduli slightly increase with an increase in  $\Omega$  from 0.3 to 0.8, suggesting that the dispersed phase of PB1 begins to have a major contribution to the dynamic storage and loss moduli of the PB1/PDMS blends. Fig. 5(a) and (b) also shows that the exponents of the power-law equation are close to 0.5 for  $\Omega \geq 0.3$ , indicating that the viscoelastic behavior of the blends is not affected by the addition of PB1 component when the weight fraction is greater than or equal to 0.3.

Fig. 6 shows the tan delta ( $\delta$ ) defined as  $\tan \delta = G''/G'$  as a function of frequency at the various concentrations of PB1 ( $\Omega=0.01, 0.1, 0.2, 0.3, 0.4, 0.5, 0.6, 0.7,$  and  $0.8$ ). It is clear



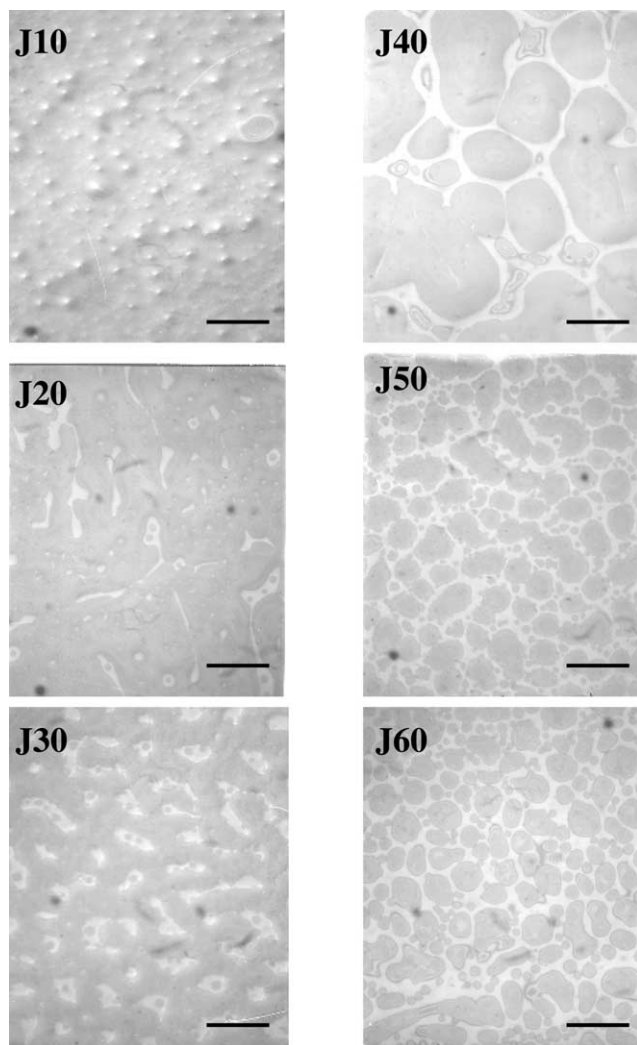


Fig. 3. Optical micrographs of PB1/PDMS blends (J-series). All scale bars are 250  $\mu\text{m}$ .

that the  $\tan \delta$  is much larger than unity over the entire frequency range for  $\Omega=0.01$  (J1), indicating that the viscous component of the modulus is dominant over its elastic counterpart. In contrast the  $\tan \delta$  is close to or smaller than 1 over the entire frequency range ( $0.1 < \omega < 100$  rad/s), indicating that the viscous component of the modulus is comparable to its elastic counterpart. It is clear that the slope in  $\tan \delta$  vs.  $\omega$  is negative over the whole range of frequency, which indicates the melt-like viscoelastic behavior. However, the slope in  $\tan \delta$  at low frequencies ( $\omega \leq 0.5$  rad/s) becomes positive (see an inset of Fig. 6), indicating the transition from melt-like to solid-like behavior [43]. This kind of solid-like viscoelastic behavior has been observed in many polymer/clay nanocomposites [26–28,44–47].

Figs. 7 and 8 show the compositional dependencies of dynamic storage modulus and loss modulus at a frequency of 0.1 rad/s for immiscible PB1/PDMS blends, respectively. A systematic increase in  $G'$  and  $G''$  is evident with an increasing PB1 weight fraction up to  $\Omega=0.3$ . The

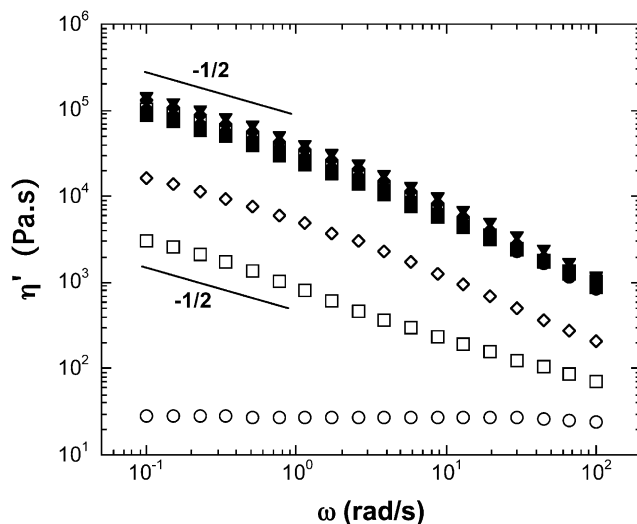


Fig. 4. Dynamic viscosity ( $\eta'$ ) of PB1/PDMS blends (J-series) without pre-shear. Symbols: J1 (circles), J10 (squares), J20 (diamonds), J30 (hatched squares), J40 (filled circles), J50 (filled squares), J60 (filled diamonds), J70 (filled triangles), J80 (reversed filled triangles).

systematic increase in the dynamic storage and loss moduli up to a critical composition ( $\Omega=0.3$ ) is due to the fact that the size of the dispersed domains (PB1 in this case) increases systematically as the concentration of PB1 in the blend increases [21,48]. In contrast the storage and loss moduli exhibit two plateaus for  $\Omega \geq 0.3$ , suggesting that the contribution of the PB1 component to the modulus is dominant and the PB1 homopolymer determines the storage and loss moduli of the PB1/PDMS blend when  $\Omega \geq 0.3$ . In particular, we note that the phase inversion composition ( $\Omega_p=0.35$ ) is larger than the point of discontinuity that would be called as a maximum weight fraction ( $\Omega_m=0.25$ ).

It has been reported that one or two peaks are appeared at low frequencies in a plot for the compositional dependence of storage or loss modulus [49–52]. The appearance of this peak is attributed to the commencement of co-continuous or bi-continuous structure due to the phase inversion. In the case of the PB1/PDMS blend, we see a peak or maximum value in the plot of  $G'$  or  $G''$  vs. composition and the onset of peak or maximum value is corresponding to the maximum weight fraction ( $\Omega_m$ ). It is very interesting and has never been reported for immiscible polymer blends that the point of discontinuity is not matched with the phase inversion composition. The compositional independencies of storage and loss moduli arise from the dominant contribution of the component PB1 to the modulus of the PB1/PDMS blend, which in turn is related to the ultrahigh viscosity ratio of the blend ( $\lambda=162,000$ ). In addition the compositional dependencies of the moduli do not follow the log-additive mixing (LAM) rule and exhibit very strong positive deviation from the LAM rule, suggesting that the storage and loss moduli are not represented by an average contribution from the dispersed and continuous phases. We also confirmed that the modulus of the blends and its discontinuity (or maximum

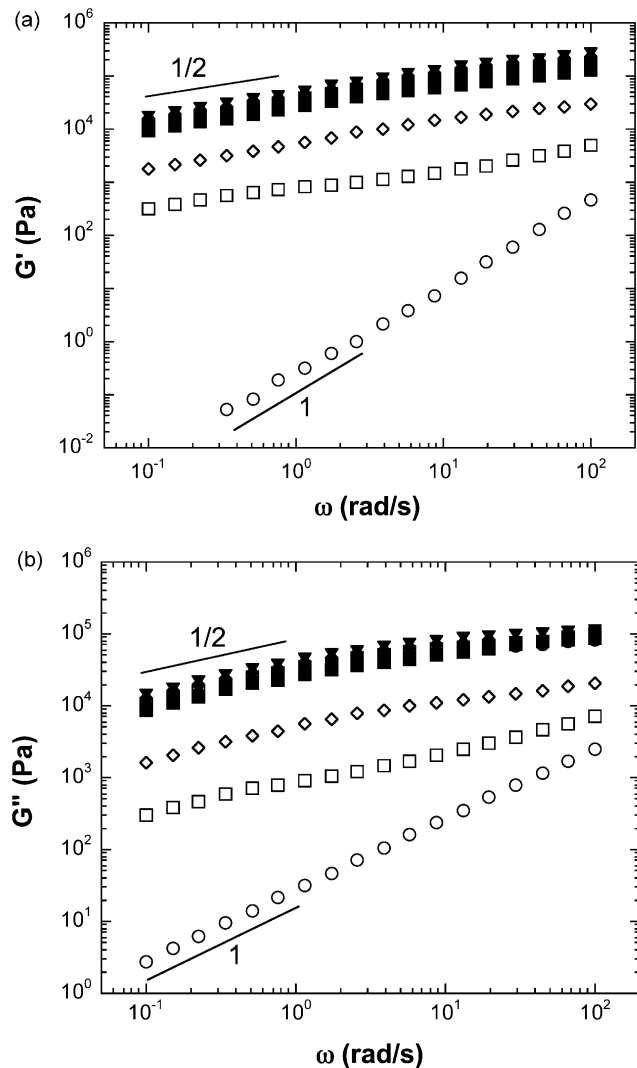


Fig. 5. (a) Dynamic storage modulus ( $G'$ ) of PB1/PDMS blends (J-series) without pre-shear. Symbols: J1 (circles), J10 (squares), J20 (diamonds), J30 (hatched squares), J40 (filled circles), J50 (filled squares), J60 (filled diamonds), J70 (filled triangles), J80 (reversed filled triangles). (b) Dynamic loss modulus ( $G''$ ) of PB1/PDMS blends (J-series) without pre-shear. Symbols: J1 (circles), J10 (squares), J20 (diamonds), J30 (hatched squares), J40 (filled circles), J50 (filled squares), J60 (filled diamonds), J70 (filled triangles), J80 (reversed filled triangles).

weight fraction) are not virtually affected with three different pre-shear conditions ( $0$ ,  $0.01$ , and  $0.1 \text{ s}^{-1}$ ).

In order to study the deformation effect of dispersed domains on the steady shear viscosity of the immiscible PB1/PDMS blends, we measured steady shear viscosity ( $\eta$ ) as a function of time at a constant shear rate  $0.1 \text{ s}^{-1}$ . Fig. 9 shows the viscosity of the blends with various compositions ( $\Omega = 0.1, 0.2, 0.3, 0.4$ , and  $0.6$ ). Below the phase inversion compositions ( $\Omega < \Omega_p$ ), the viscosity of the deformed blends (J10, J20, and J30) with a PB1-dispersed phase decreases at  $t < \sim 200 \text{ s}$ . The decrease in the viscosity is probably due to the deformation of the dispersed PB1 domains in the immiscible PB1/PDMS blend since the breakup of dispersed

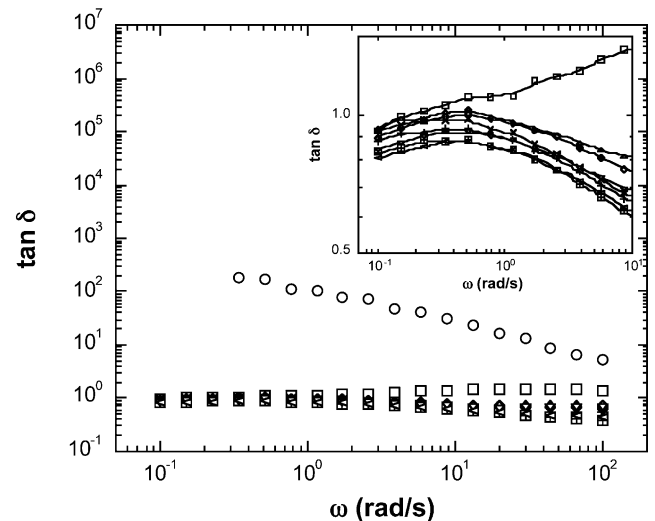


Fig. 6. Dynamic  $\tan \delta$  of PB1/PDMS blends (J-series). Symbols: J1 (circles), J10 (squares), J20 (diamonds), J30 (crosses), J40 (pluses), J50 (triangles), J60 (hatched squares), J70 (reversed triangles), J80 (tilted triangles). Inset: An enlarged figure to look at the transition from melt-like to solid-like behavior in the lower frequency region ( $0.1 < \omega < 10 \text{ rad/s}$ ).

domains in shear flow is not possible if the viscosity ratios above 4 [23]. The similar behavior has been reported for polydiene blends [24,48,53]. Above the phase inversion ( $\Omega > \Omega_p$ ), however, the J40 and J60 blends with a PDMS-dispersed phase exhibit almost time-independent constant values of viscosity, suggesting the viscosity of these blends are not affected by the breakup and/or deformation of dispersed PDMS domains.

The steady shear given to the PB1/PDMS blends does not affect the viscosity to a significantly noticeable extent for the J40 and J60 blends whereas it reduces the viscosity of the J10, J20, and J30 blends. This could be explained by

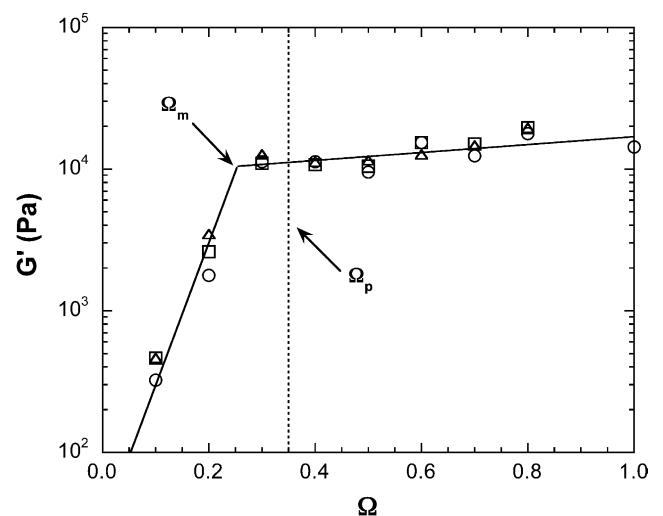


Fig. 7. Compositional dependence of dynamic storage modulus ( $G'$ ) of PB1/PDMS blends (J-series) at three different pre-shear rates. The labels  $\Omega_m$  and  $\Omega_p$  are maximum and phase inversion weight fraction of PB1 in the PB1/PDMS blends, respectively. Symbols: without pre-shear (circles), pre-shear  $0.01 \text{ s}^{-1}$  (squares), and pre-shear  $0.1 \text{ s}^{-1}$  (triangles).

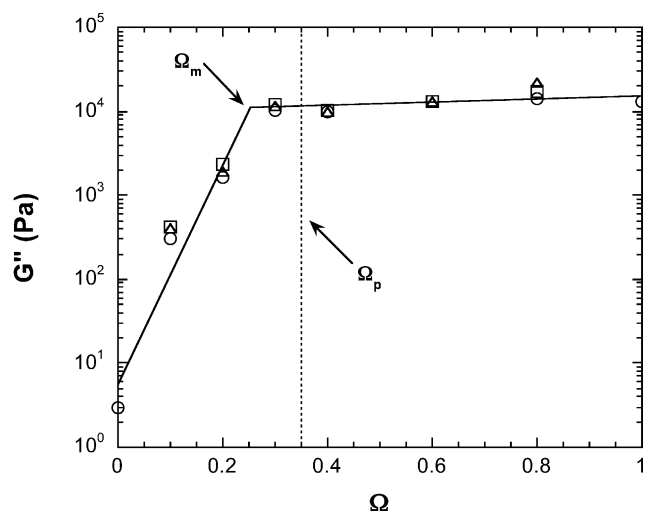


Fig. 8. Compositional dependence of dynamic loss modulus ( $G''$ ) of PB1/PDMS blends (J-series) at three different pre-shear rates. The labels  $\Omega_m$  and  $\Omega_p$  are maximum and phase inversion weight fraction of PB1 in the PB1/PDMS blends, respectively. Symbols: without pre-shear (circles), pre-shear  $0.01 \text{ s}^{-1}$  (squares), and pre-shear  $0.1 \text{ s}^{-1}$  (triangles).

dwelling on an extended version of Taylor’s theory [54,55] that the deformation of the dispersed domains depends on the interfacial tension between continuous and dispersed phases as well as the externally induced flow characteristics. If the dispersed phase is more viscous than the continuous phase, the external flow would be an only governing factor for the deformation of the droplet [56]. Nevertheless, the effects due to the external flow on the deformation of dispersed domains are negligible for the phase inverted J40 and J60 blends, where the less viscous PDMS is dispersed phase while the more viscous PB1 is continuous phase and the viscosity ratio is extremely small,  $\lambda = 1/162,000$ .

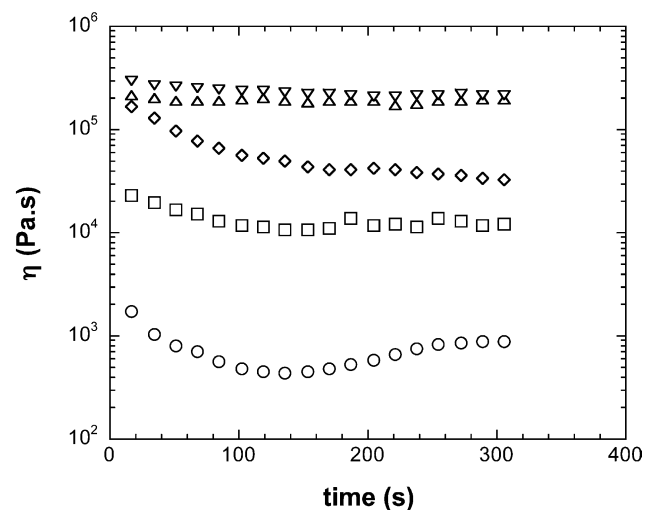


Fig. 9. Steady shear viscosity of PB1/PDMS blends (J-series). Symbols: J10 (circles), J20 (squares), J30 (diamonds), J40 (triangles), and J60 (reversed triangles).

### 3.3. PB2/PDMS blends with high viscosity ratio ( $\lambda=37$ )

Fig. 10 shows optical micrographs of two-phase PB2/PDMS blends under quiescent conditions. The dispersed phase of PB2 appears as bright domains while the continuous PDMS phase is shown as dark color in the K10, K30, and K50 blends. In contrast the dispersed PDMS domains are shown as dark color and have a broad size distribution in the K90 blends. In particular, the K70 blend shows more complicated morphology; the dispersed phase shows the bright domains with dark rims while the bicontinuous-like matrix phase having mixed colors of dark and bright is shown as a background image. We thus determine the phase inversion composition as  $\Omega_p=0.7$  for the PB2/PDMS blends (K-series) at a quiet pre-shear condition. It is clear that the dispersed phase is shown as bright PB2 domains up to the phase inversion composition.

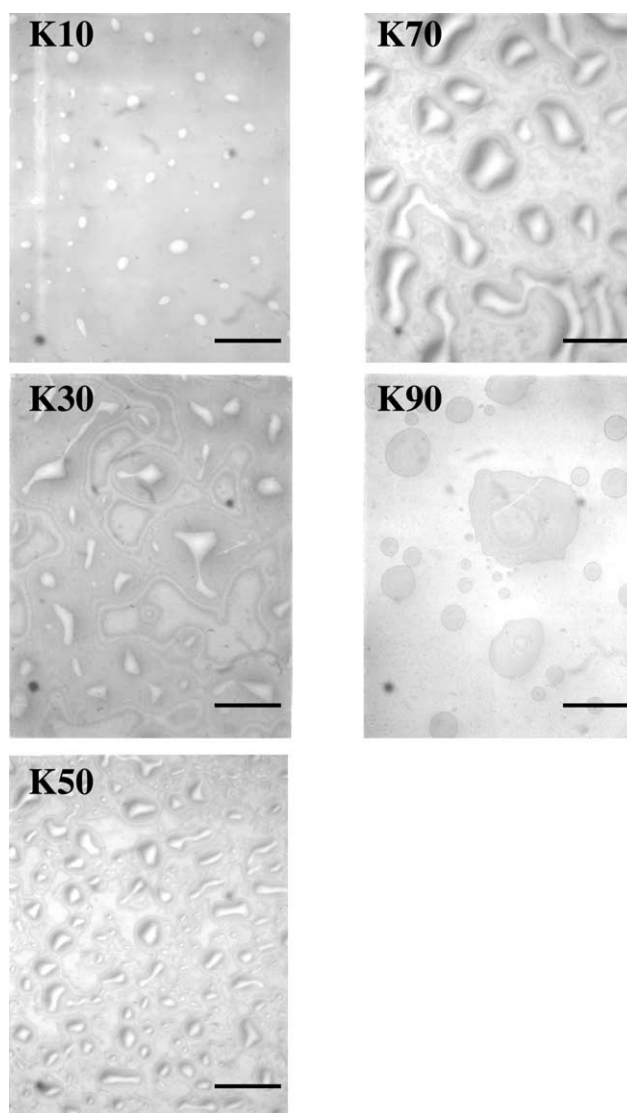


Fig. 10. Optical micrographs of PB2/PDMS blends (K-series). All scale bars are 250  $\mu\text{m}$ .

Fig. 11 shows the dynamic viscosity ( $\eta'$ ) of the immiscible PB2/PDMS blends for a wide range of PB2 weight fractions (0.1–0.9). The blends (K10, K30, and K50) exhibit Newtonian fluids behavior at all frequencies, while the K70 and K90 blends are characterized as very weak shear-thinning fluids over all frequencies tested in this work ( $0.1 < \omega < 100$  rad/s).

Fig. 12(a) and (b) shows the storage and loss moduli for the immiscible PB2/PDMS blend at the various weight fraction of PB2 ( $\Omega = 0.1, 0.3, 0.5, 0.7,$  and  $0.9$ ). We see a systematic increase in both  $G'$  and  $G''$  until  $\Omega \leq 0.7$ . There are big jumps in modulus for  $W = 0.7$ , while relatively small increases in loss modulus compared to those of the K50 blend in the terminal regime. Interestingly, the storage modulus decreases while the loss modulus slightly increases with an increase in  $\Omega$  from 0.7 to 0.9. Also, the exponents of the power-law equation in the storage modulus of the blends are much smaller than 1.0 for all blends, indicating that the interfacial force between two phases has a non-negligible contribution to the storage modulus of the blends. If the blends are immiscible or phase-separated, the exponent values in the storage and loss moduli are typically less than 2.0 and 1.0 in the terminal regime, respectively. It has been reported that the experimental values of the power-law exponents in the terminal regime of  $G'$  vary between 0.5 and 1 for polydispersed homopolymer [57], two-phase polymer blends [24,48,58], diblock copolymers [59–61], and polymer-clay nanocomposites [27,28,44–47]. In contrast to the storage modulus, the loss modulus shows a typical value of 1.0 for all concentrations. The loss modulus has been shown to be either insensitive or less sensitive [27,28,62] to the interface of phase separated or immiscible polymer blends.

Figs. 13 and 14 show the compositional dependencies of the dynamic storage and loss moduli at a frequency of 0.1 rad/s for the immiscible PB2/PDMS blends, respectively. A systematic increase in  $G'$  and  $G''$  with an increasing

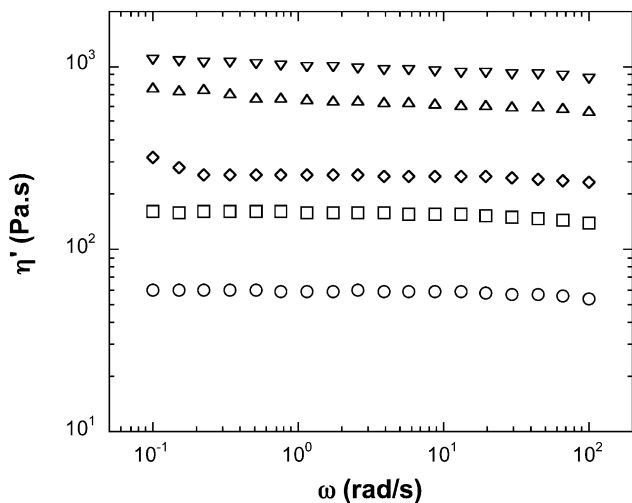


Fig. 11. Dynamic viscosity ( $\eta'$ ) of PB2/PDMS blends (J-series) without a pre-shear. Symbols: K10 (circles), K30 (squares), K50 (diamonds), K70 (triangles), k900 (reversed triangles).

PB2 weight fraction is clearly shown up to the phase inversion,  $\Omega_p = 0.7$ , and the discontinuity observed in the plot of  $G'$  vs.  $\Omega$  and  $G''$  vs.  $\Omega$  is observed at  $\Omega = \Omega_p$ . Moreover, the storage modulus decreases dramatically whereas the loss modulus increases slightly with an increasing  $\Omega$  from 0.7 to 1. This means that the viscoelastic contribution due to the interfaces between PB2 and PDMS phases is comparable to those of each component before and after phase inversion in the case of the PB2/PDMS (K-series) blends. In contrast to the PB1/PDMS (J-series) blends, the phase inversion ( $\Omega_p = 0.7$ ) is exactly matched to the point of discontinuity ( $\Omega_m = 0.7$ ) in the compositional dependence of the storage and loss moduli in the PB2/PDMS (K-series) blends.

#### 4. Concluding remarks

We have conducted a systematic study of the rheological properties, morphology, and phase inversion of two immiscible polymer blends of PB1/PDMS and PB2/PDMS. The PB2 and PDMS homopolymers exhibit Newtonian fluids behavior while a high viscosity PB1 homopolymer exhibits non-Newtonian fluids behavior. The addition of an ultrahigh viscosity polymer PB1 to the matrix of a very low viscosity polymer PDMS has resulted in the formation of polymer nanocomposite-like blends with an ultrahigh viscosity ratio ( $\lambda = 162,000$ ) and its viscoelastic behavior is similar to those of polymer/clay nanocomposites.

Though we have two immiscible blends (J- and K-series) with very high viscosity ratios, we have observed very distinct viscoelastic behavior as well as unusual structure–property relationships, such as a mismatch between phase inversion and discontinuity in the J-series blend. We have identified the phase inversion compositions of two immiscible J- and K-series blends as  $\Omega_p = 0.35$  and  $0.7$ , respectively, by using optical microscope. Also, we have determined the point of discontinuity in the storage and loss moduli as 0.25 (J-series) and 0.7 (K-series) by using rheological methods [5,24]. We should note that these two critical points of phase inversion and discontinuity are not identical for the PB1/PDMS blend (J-series) while we see an exact match for the PB2/PDMS blend (K-series). In particular, the viscoelastic properties of the PB1/PDMS blend exhibit plateaus and these values are identical to those of PB1 in case of  $\Omega > \Omega_m$ .

In regards to the mismatch between  $\Omega_m$  and  $\Omega_p$  for the PB1/PDMS blends, the reason for the discontinuity in the compositional dependence of the viscoelastic properties could not be attributed to the breakup of a dispersed phase nor the phase inversion because, when the viscosity ratio of a polymer blend is greater than 4, the highly viscous dispersed domains are too viscous to be substantially deformed by a low viscous matrix, and thus the breakup with steady or oscillatory shear is hampered [63–65]. In this case, the flow field of a low viscous PDMS matrix is not able



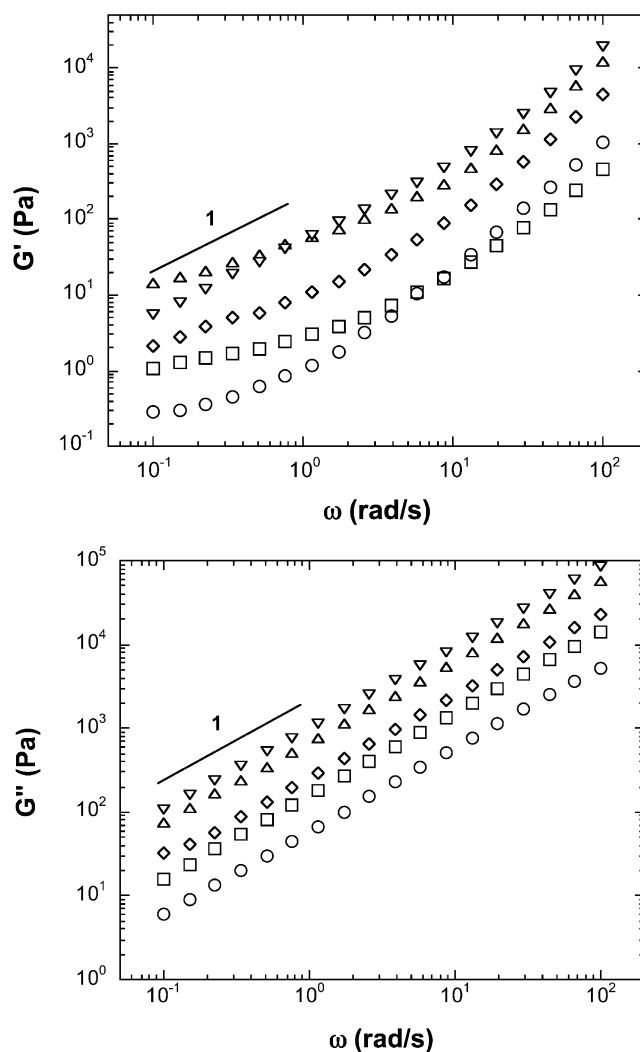


Fig. 12. (a) Dynamic storage modulus ( $G'$ ) of PB2/PDMS blends (K-series) without pre-shear. Symbols: K10 (circles), K30 (squares), K50 (diamonds), K70 (triangles), K90 (reversed triangles). (b) Dynamic loss modulus ( $G''$ ) of PB2/PDMS blends (K-series) without pre-shear. Symbols: K10 (circles), K30 (squares), K50 (diamonds), K70 (triangles), K90 (reversed triangles).

to sufficiently transfer the applied shear stresses to the highly viscous dispersed phase of PB1.

In addition the droplet size is almost invariant during the dynamic shear measurements if the strain amplitude ( $\gamma$ ) is less than 0.25 [65] or the viscosity ratio ( $\lambda$ ) of polymer blends is greater than  $\sim 4$  [21,66], which are both the cases in our experiments ( $\gamma=0.1$  and  $\lambda \gg 4$ ). In order to attain a good dispersion in a physical mixing process of immiscible polymer blends, the dynamic and viscous forces acting on the surface of a small domain during shear will tend to break or deform it. In contrast, the interfacial tension between the matrix and the dispersed phase will tend to resist these forces to maintain the shape of domain. When the dynamic and viscous forces become larger than the interfacial forces, the domain deforms and eventually breaks into smaller domains. But if the interfacial forces exceed the dynamic and the viscous forces there would be the coalescence of domains [12,67–69] although the domain sizes were not

affected by the pre-shear owing to the very high viscosity ratio of the blends [69].

However, in the case of polymer blends with a low viscosity ratio ( $\lambda < 4$ ), the pre-shear may determine the domain size of the J-series and K-series blends with  $\Omega > \Omega_p$ . The higher pre-shear rate will produce the smaller domain size [70]. In contrast, in our J-series blends, the viscosity ratio of the blend becomes very much smaller than 4 after phase inversion, which means that the domain size of the dispersed PDMS phase could be broken up into smaller domains. But the viscoelastic properties of the PB1/PDMS blends having PDMS domains (J40, J50, J60, J70, and J80) are not affected by the breakup of the dispersed PDMS domains. This is probably due to the ultrahigh asymmetry in the viscosity of the blend components and the very strong contribution of the higher viscosity PB1 component to the viscoelastic properties of the blends.

In this paper, we have attempted to demonstrate the effects of ultrahigh viscous asymmetry on the structure–property

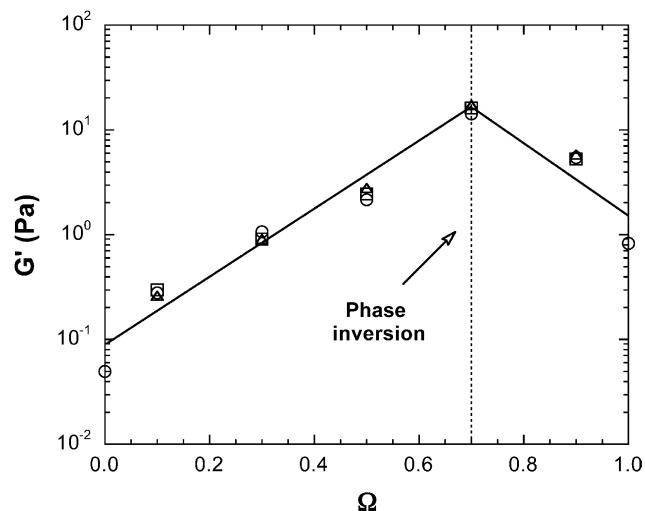


Fig. 13. Compositional dependence of the dynamic storage modulus ( $G'$ ) of PB2/PDMS blends (K-series) at three different pre-shear rates. Symbols: without pre-shear (circles), pre-shear  $0.01 \text{ s}^{-1}$  (squares), and pre-shear  $0.1 \text{ s}^{-1}$  (triangles).

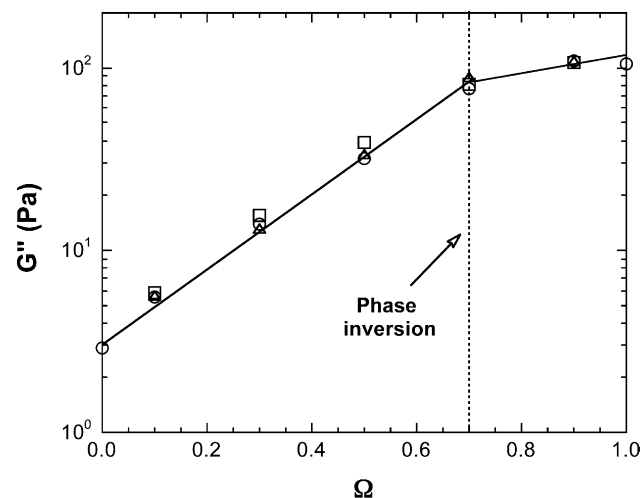


Fig. 14. Compositional dependence of dynamic loss modulus ( $G''$ ) of PB2/PDMS blends (K-series) at three different pre-shear rates. Symbols: without pre-shear (circles), pre-shear  $0.01 \text{ s}^{-1}$  (squares), and pre-shear  $0.1 \text{ s}^{-1}$  (triangles).

relationships of immiscible polymer blends with rheological and morphological approaches, and we hope that this work will motivate to develop advanced polymer nanocomposite-like multi-phase materials.

### Acknowledgements

This study was financially supported by special research fund of Chonnam National University in 2004.

### References

- [1] Han CD. Multiphase flow in polymer processing. New York: Academic Press; 1981.
- [2] Utracki LA. Polymer alloys and blends. New York: Hanser Publishers; 1990.
- [3] Paul DR. In: Paul DR, Newman S, editors. Polymer blends, vol. 1. New York: Academic Press; 1978.
- [4] Jeon HS, Lee JH, Balsara NP, Majumdar B, Fetters LJ, Faldo A. *Macromolecules* 1997;30:973.
- [5] Wang ZG, Safran SA. *J Phys (Paris)* 1990;51:185.
- [6] Jeon HS, Kim S, Han CC. *J Polym Sci, Part B: Polym Phys* 2001;39:819.
- [7] Roe RJ, Rigby D. *Adv Polym Sci* 1987;82:103.
- [8] Cohen RE, Ramos AR. *Macromolecules* 1979;12:131.
- [9] Lohse DJ, Datta S, Kresge EN. *Macromolecules* 1991;24:561.
- [10] Lee JH, Ruegg ML, Balsara NP, Zhu YQ, Gido SP, Krishnamoorti R, et al. *Macromolecules* 2003;36:6537–48.
- [11] Han MS, Seo WJ, Paik HS, Hyun JC, Lee JW, Kim WN. *Polym J* 2003;35(2):127–32.
- [12] Wang P, Koberstein JT. *Macromolecules* 2004;37(15):5671–81.
- [13] Lin B, Sundararaj U. *Polymer* 2004;45(22):7605–13.
- [14] Oyama HT, Kitagawa T, Ougizawa T, Inoue T, Weber M. *Polymer* 2004;45(3):1033–43.
- [15] Deyrail Y, Cassagnau P. *J Rheol* 2004;48(3):505–24.
- [16] Castro M, Carrot C, Prochazka F. *Polymer* 2004;45:4095–104.
- [17] Gramespacher H, Meissner J. *J Rheol* 1992;36:1127.
- [18] Kernick WA, Wagner NJ. *J Rheol* 1999;43:521.
- [19] Minale M, Moldenaers P, Mewis J. *J Rheol* 1999;43:815.
- [20] Vinckier I, Minale M, Mewis J, Moldenaers P. *Colloids Surf* 1999;150:217.
- [21] Vinckier I, Moldenaers P, Mewis J. *J Rheol* 1996;40:613.
- [22] Valenza A, Lyngaae-Jorgensen J, Utracki LA, Sammut P. *Polym Networks Blends* 1991;1:79.
- [23] Grace HP. *Chem Eng Commun* 1982;14:225.
- [24] Jeon HS, Nakatani AI, Han CC, Colby RH. *Macromolecules* 2000;33:9732.
- [25] Ferry JD. *Viscoelastic properties of polymers*. 2nd ed. New York: Wiley; 1970 (chapter 1).
- [26] Pinnavaia TJ, Beall GW, editors. *Polymer–clay nanocomposites*. New York: Wiley; 2001.
- [27] Jeon HS, Rameshwaram JK, Kim G, Weinkauff DH. *Polymer* 2003;44:5749.
- [28] Jeon HS, Rameshwaram JK, Kim G. *J Polym Sci, Part B: Polym Phys* 2004;42:1000.
- [29] Rachapudy H, Smith GG, Raju VR, Graessley WW. *J Polym Sci, Polym Phys Ed* 1979;17:1211.
- [30] Morton M, Fetters LJ. *Rubber Chem Technol* 1975;48:359.
- [31] Akay G. *Chem Eng Sci* 1998;53:203.
- [32] Tanaka H, Araki T. *Phys Rev Lett* 1997;78:4966.
- [33] De Roover B, Devaux J, Legras R. *J Polym Sci, A: Polym Chem* 1997;35:917.
- [34] Mekhilef N, Verhoogt H. *Polymer* 1996;37:4069.
- [35] Barton BF, Reeve LL, McHugh AJ. *J Polym Sci, Part B: Polym Phys* 1997;35:569.
- [36] Paul DR, Barlow J. *J Macromol Sci, Rev Macromol Chem* 1980;C18:109.
- [37] Jordhamo GM, Manson JA, Spering LH. *Polym Eng Sci* 1986;26:517.
- [38] Miles IS, Zurek A. *Polym Eng Sci* 1988;28:796.
- [39] Bouilloux A, Ernst B, Lobbrecht A, Muller R. *Polymer* 1997;38:4775.
- [40] Favis BD, Chalifoux JP. *Polymer* 1988;29:1761.
- [41] Hobbie EK, Jeon HS, Wang H, Kim H, Stout DJ, Han CC. *J Chem Phys* 2002;117:6350.
- [42] Jeon HS, Shou Z, Chakrabarti A, Hobbie K. *Phys Rev E* 2002;65:41508.
- [43] Winter HH, Mours M. *Adv Polym Sci* 1997;134:166–233.
- [44] Giannelis EP, Krishnamoorti R, Manias E. *Adv Polym Sci* 1999;138:107 [and references therein].
- [45] Hoffmann B, Kressler J, Stoppelmann G, Friedrich Chr, Kim GM. *Colloid Polym Sci* 2000;278:629.
- [46] Lepoittevin B, et al. *Polymer* 2002;43:4017.

- [47] Jeon HS, Rameshwaram JK. In: Mammoli AA, Brebbia CA, editors. Computational methods in materials characterization, Section 7. UK: WIT Press; 2003.
- [48] Jeon HS, Nakatani AI, Hobbie EK, Han CC. *Langmuir* 2001;17:3087.
- [49] Galloway JA, Macosko CW. *Polym Eng Sci* 2004;44(4):714–27.
- [50] Huitri J, Mederic P, Moan M, Jarrin J. *Polymer* 1998;39:4849–56.
- [51] Steinmann S, Gronski W, Freidrich C. *Polymer* 2001;42:6619–29.
- [52] Steinmann S, Gronski W, Freidrich C. *Rheol Acta* 2002;41:77–86.
- [53] Jeon HS, Hobbie EK. *Phys Rev E* 2001;63:61403.
- [54] Taylor GI. *Proc R Soc London, Ser A* 1932;138:41–8.
- [55] Taylor GI. *Proc R Soc London, Ser A* 1934;146:501–23.
- [56] Lee HM, Park OO. *J Rheol* 1994;38(5):1405–25.
- [57] Mani S, Malone MF, Winter HH, Halary JL, Monnerie L. *Macromolecules* 1991;24:5451.
- [58] Eckstein A, Friedrich Chr, Lobbrecht A, Spitz R, Mulhaupt R. *Acta Polym* 1997;48:41.
- [59] Rosedale JH, Bates FS. *Macromolecules* 1990;23:2329.
- [60] Rosedale JH, Bates FS, Almdal K, Mortensen K, Wignall GD. *Macromolecules* 1995;28:1429.
- [61] Stuhn B, Mutter R, Albrecht T. *Europhys Lett* 1992;18:427.
- [62] Vaia RA, Ishii H, Giannelis EP. *Chem Mater* 1993;5:1694.
- [63] Janssen JMH, Meijer HEH. *J Rheol* 1993;37:597–608.
- [64] Everaert V, Aerts L, Groeninckx G. *Polymer* 1999;40:6627–44.
- [65] Scott CE, Joung SK. SPE Retec symposium on polymer alloys and blends, Boucherville, Canada, proceedings 1995. p. 338.
- [66] Kitade S, Ichikawa A, Imura N, Takahashi Y, Noda I. *J Rheol* 1997;41(5):1039–60.
- [67] Lyoo WS, Choi YG, Choi JH, Ha WS, Kim BC. *Int Polym Process XV* 2000;4:369.
- [68] Tokita N. *Chem Technol* 1977;50:292.
- [69] Vinckier I, Minale M, Mewis J, Moldenaers P. *Colloids Surf A: Physicochem Eng Aspects* 1999;150:217–28.
- [70] Graebing D, Muller R, Palierne JF. *Macromolecules* 1993;26:320–9.